AIP Applied Physics Letters

Multi-stack InAs/InGaAs sub-monolayer quantum dots infrared photodetectors

J. O. Kim, S. Sengupta, A. V. Barve, Y. D. Sharma, S. Adhikary et al.

Citation: Appl. Phys. Lett. **102**, 011131 (2013); doi: 10.1063/1.4774383
View online: http://dx.doi.org/10.1063/1.4774383
View Table of Contents: http://apl.aip.org/resource/1/APPLAB/v102/i1
Published by the American Institute of Physics.

Related Articles

Operation of a titanium nitride superconducting microresonator detector in the nonlinear regime
J. Appl. Phys. 113, 104501 (2013)

Modeling of the infrared photodetector based on multi layer armchair graphene nanoribbons
J. Appl. Phys. 113, 093106 (2013)

Theoretical investigation of InAs/GaSb type-II pin superlattice infrared detector in the mid wavelength infrared range
J. Appl. Phys. 113, 083717 (2013)

Electrical detection of surface plasmon resonance phenomena by a photoelectronic device integrated with gold nanoparticle plasmon antenna
Appl. Phys. Lett. 102, 083702 (2013)

Effects of annealing temperature on the characteristics of Ga-doped ZnO film metal-semiconductor-metal ultraviolet photodetectors
J. Appl. Phys. 113, 084501 (2013)

Additional information on Appl. Phys. Lett.

Journal Homepage: http://apl.aip.org/
Journal Information: http://apl.aip.org/about/about_the_journal
Top downloads: http://apl.aip.org/features/most_downloaded
Information for Authors: http://apl.aip.org/authors

ADVERTISEMENT

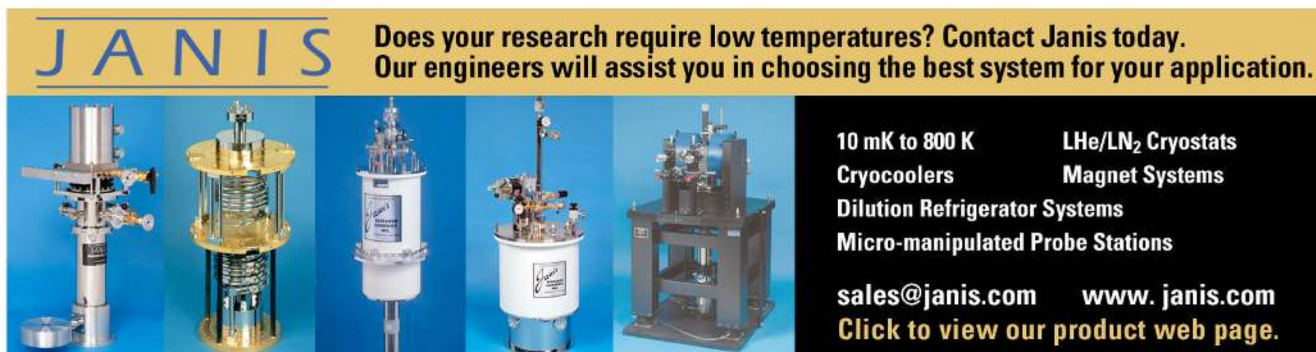

Downloaded 09 Mar 2013 to 139.184.30.132. Redistribution subject to AIP license or copyright; see http://apl.aip.org/about/rights_and_permissions

APPLIED PHYSICS LETTERS 102, 011131 (2013)

Multi-stack InAs/InGaAs sub-monolayer quantum dots infrared photodetectors

J. O. Kim,[1] S. Sengupta,[2] A. V. Barve,[1] Y. D. Sharma,[1] S. Adhikary,[2] S. J. Lee,[3] S. K. Noh,[3,a)] M. S. Allen,[4] J. W. Allen,[4] S. Chakrabarti,[2] and S. Krishna[1,a)]
[1]*Department of Electrical and Computer Engineering, Center for High Technology Materials, University of New Mexico, Albuquerque, New Mexico 87106, USA*
[2]*Department of Electrical Engineering, Center for Nanoelectronics, Indian Institute of Technology Bombay, Mumbai-400076, India*
[3]*Korean Research Institute of Standards and Science, Daejeon 305-340, South Korea*
[4]*Sensors Directorate, Air Force Research Laboratory, WPAFB, Ohio 45433, USA*

(Received 27 August 2012; accepted 20 December 2012; published online 11 January 2013)

We report on the design and performance of multi-stack InAs/InGaAs sub-monolayer (SML) quantum dots (QD) based infrared photodetectors (SML-QDIP). SML-QDIPs are grown with the number of stacks varied from 2 to 6. From detailed radiometric characterization, it is determined that the sample with 4 SML stacks has the best performance. The s-to-p (s/p) polarized spectral response ratio of this device is measured to be 21.7%, which is significantly higher than conventional Stranski-Krastanov quantum dots (∼13%) and quantum wells (∼2.8%). This result makes the SML-QDIP an attractive candidate in applications that require normal incidence. © *2013 American Institute of Physics*. [http://dx.doi.org/10.1063/1.4774383]

Quantum dot (QD) systems have attracted a lot of interest not only in the exploration of basic properties[1] but also in applications of optoelectronic devices, such as QD-based laser diodes,[2,3] infrared photodetectors,[4,5] single photon emitters,[6] and single-electron devices.[7] Various techniques have been used for the growth of QD structures. These include the formation of self-assembled QD, for example, Stranski-Krastanov (SK) growth mode,[8,9] atomic layer epitaxy (ALE) growth mode,[10,11] and droplet epitaxy growth mode.[12] The sub-monolayer-quantum dots (SML-QD) system is one of the few technologies that may provide an attractive alternative to the formation of QD using self-assembly techniques. The absence of a wetting layer can improve confinement in SML-QD and the reduction in the amount of InAs used per layer of QD can help stack more layers in a 3-dimensional QD structure. Several groups have reported using SML QD in vertical cavity surface-emitting lasers[13] and disk lasers.[14]

Quantum dot infrared photodetectors (QDIPs) based on SK-QD have been widely researched in recent years and have been used to fabricate focal plane arrays. Many research groups have been working on methods to improve the QDIP device performance by changing the composition of the QD (e.g., InAs, InGaAs, InAlGaAs) and by changing the design of the structure (e.g., quantum dots in-a-well: DWELL,[15,16] quantum dots in double well: DDWELL,[17] quantum dot in-a-well with confinement enhancing (CE) barriers: CE DWELL[18] and resonant tunneling heterostructure[19]). SK-QDIPs have been demonstrated at high operating temperature in imaging application for the mid-infrared regime. However, compared to the number of dopants in the active regions of quantum well (QW) infrared photodetectors (QWIP), size variation in dot structures and low QD density in QDIPs fabricated using SK growth mode, limit the absorption quantum efficiency (QE). Therefore, improving QD uniformity and density is a key to increasing absorption QE and normal incidence absorption, thereby improving the overall device performance. Recently, Ting *et al*. reported promising results for a 1024×1024 pixels SML-QDIP focal plane array camera used to acquire an infrared image at 80 K.[20]

SML-QDs have several advantages over SK-QDs including smaller base diameter (5–10 nm), better 3D quantum confinement, higher dot density ($\sim 5 \times 10^{11}\,\mathrm{cm}^{-2}$), adjustable height of the dot geometry, and no wetting layer needed.[21] The absence of a wetting layer, which does not contribute to the normal incidence absorption, and smaller base diameter lead to stronger in-plane quantum confinement when compared to SK-QDs. Typically, InAs SML-QD consists of a stacked deposition of the QD materials with a normal thickness below one monolayer (1 ML) in a (In)GaAs QW.[22]

In this letter, we present results for SML-QD based QDIP devices fabricated using a multi-stack growth technique. Device characteristics, including spectral response, detectivity, and absorption quantum efficiency of five types of devices with different SML-QD stacks are analyzed and compared to those of SK-QD. We also compare the s-to-p (s/p) polarized spectral response with devices based on SK-QD, SML-QD, and QW, as measured with the ratio of 13%, 22%, and 2.8%, respectively.

The devices were grown using molecular beam epitaxy (MBE) with As_2 cracker source on a semi-insulating GaAs [0 0 1] substrate. The active region has a single period that consists of a multiple stacks of 0.3 ML InAs SML-QDs embedded in $In_{0.15}Ga_{0.85}As$ QW (5.3 nm thick) surrounded by GaAs (1 nm thick), $Al_{0.22}Ga_{0.78}As$ confinement enhancing barrier (2 nm thick), and $Al_{0.07}Ga_{0.93}As$ barriers (48 nm thick) as shown in Fig. 1. This CE DWELL structure has been previously reported by our group[18] using 2.0 ML

a)Authors to whom correspondence should be addressed. Electronic addresses: skrishna@chtm.unm.edu. and sknoh@kriss.re.kr.

 © 2013 American Institute of Physics

Downloaded 09 Mar 2013 to 139.184.30.132. Redistribution subject to AIP license or copyright; see http://apl.aip.org/about/rights_and_permissions

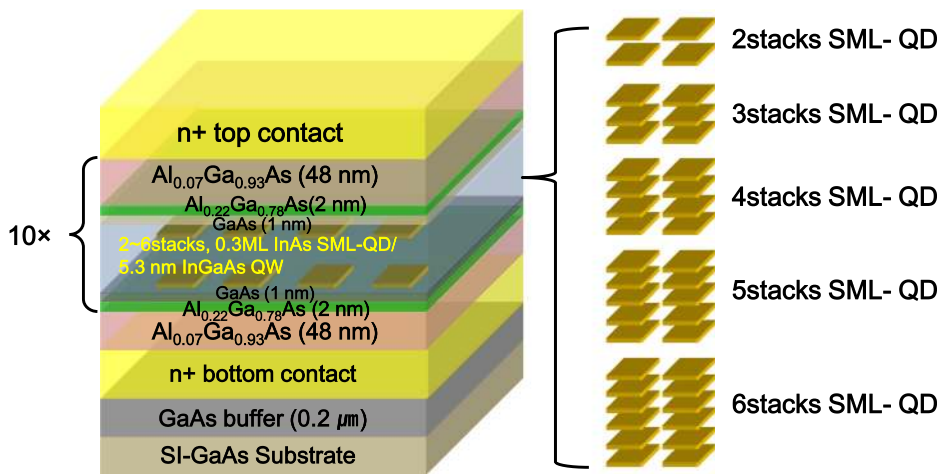

FIG. 1. Heterostructure schematic of multiple stacked SML-QD. 0.3 ML InAs SML-QDs with 2–6 stacks embedded in a 5.3 nm $In_{0.15}Ga_{0.85}As$ QW.

SK-QDs instead of SML-QDs. A 200 nm buffer layer, 600 nm bottom contact layer, 48 nm $Al_{0.07}Ga_{0.93}As$ barrier, and 2 nm $Al_{0.22}Ga_{0.78}As$ CE barrier were grown and capped with 1 nm GaAs layer at 590 °C. The substrate temperature was then cooled to 500 °C to grow the InGaAs QW and 2–6 stacks SML-QDs doped with Si. The As interruption time was 10 s before and after each of 0.3 ML InAs layer deposition during the formation of the SML-QD stack. The QW layer was capped with 1 nm GaAs before changing the substrate temperature at 590 °C. The devices were processed in $410 \times 410\,\mu m^2$ mesas using inductively coupled plasma etching, followed by the contact metal deposition. The devices had a circular aperture of 300 μm in each mesa.

Figure 2(a) shows the data comparison for normal incidence spectral response measured for SK-QDIP and five SML-QDIPs, where the number of stacks was varied from 2 to 6. The control sample using conventional SK growth mode had two peaks in the spectral response at 6.5 μm and 7.5 μm. As indicated in the inset of Fig. 2(a), the first peak (6.5 μm) can be attributed to an intersubband transition from the ground state and the second peak (7.5 μm) can result from a transition from the excited state of the QDs to the excited state of the QW.[18] As shown in Fig. 2(b), SML-QDIP consisting of 4–6 stacks of SML-QDs exhibit a peak at 7.5 μm due to transition between the ground state of SML-QD and the excited state of QW (bound to bound transition: B-B transition), resulting in narrow spectral response. The single peak of spectral response can be related to the size and uniformity of QDs. SK-QDs have both a ground state and an excited state, while SML-QDs have only the ground state due to smaller QD size than SK-QDs. The devices consisting of 2–3 stacks of SML-QDs show a red-shift and broad spectral response as compared to devices consisting of 4–6 stacks of SML-QDs. The broad spectral response of 2–3 stack devices is a result of bound to quasi-bound (B-Q) transition since the excited state of QW is close to the continuum energy level, as shown in Fig. 2(b). For 2 stacks SML-QDs, indicated by a blue-shift in photoluminescence (PL) by $\sim$100 meV as compared to the 6 stacks SML-QDs (not shown here), both QD's ground state energy and the QW's excited state energy are higher. This B-Q transitions result in a red-shift in spectral response. Note that the schematic of conduction band diagram of SML-QDIPs is not based on simulation, but is based on semi-empirical estimates from the PL measurements.

The detectivity (D*) as a function of bias voltage for each device at 77 K was also compared (see Fig. 3(a)). For SML-QDIP, the highest D* value measured was 1.2×10^{11} cm·Hz$^{1/2}$ W^{-1} (at 77 K, 0.4 V, 7.5 μm, *f*/2) for the 4 stacks SML-QDIP device. The results of D* show that as the number of SML-QD stacks increases, the value of D* increases up to 4 stacks. The value shows a decreasing trend as the number of SML stacks is increased beyond 4. The dark current in 2–3 stack devices is much higher as

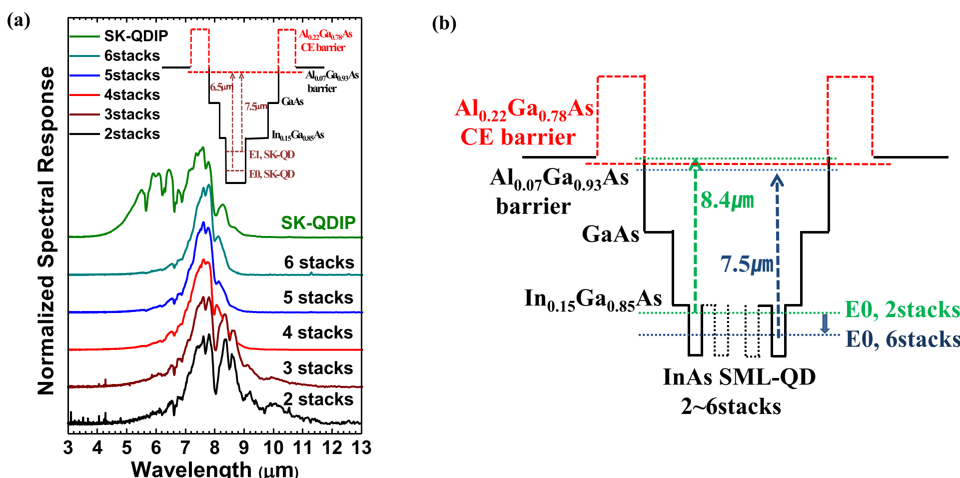

FIG. 2. (a) Comparison of spectral response between the SML-QDIP with different stacks QD and the SK-QDIP device at 77 K. Inset shows the schematic of transition of SK-QDIP. (b) Schematic conduction band diagram of 2–6 stacks SML-QDIP.

Downloaded 09 Mar 2013 to 139.184.30.132. Redistribution subject to AIP license or copyright; see http://apl.aip.org/about/rights_and_permissions

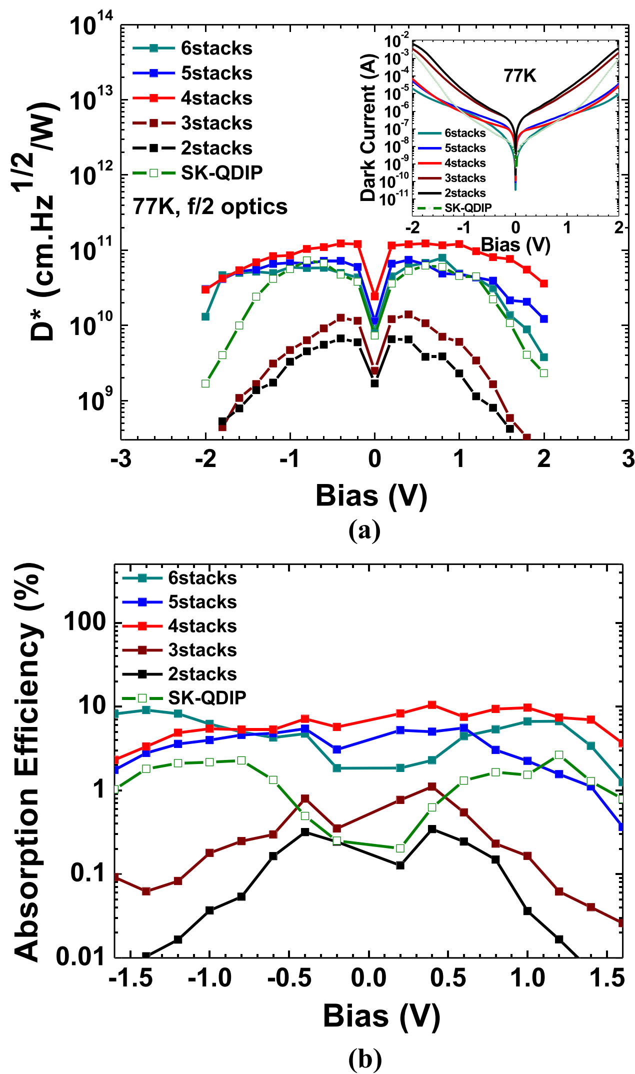

FIG. 3. (a) Comparison of measured detectivity between the SML-QDIP and the SK-QDIP device at 77 K (f/2 optics), showing the highest value for 4 stacks SML-QDIP. Inset shows the dark current at 77 K. (b) Absorption quantum efficiency of each device is shown.

compared to the 4-6 stack devices, as shown in the inset of Fig. 3(a). The lower dark current of 4–6 stacks SML-QDIP could be owing to the improved crystal quality and better quantum confinement. We believe that the crystal quality of SML-QD is associated with the thickness of spacer between stack and stack due to the vertical coupling of each stack QD. Therefore, the thickness of InGaAs QW between stacks is expected to depend on stack numbers for better device performance. Specifically, decreasing (increasing) the spacer thickness in 2, 3 stacks (5, 6 stacks) would result in better performance. For SK-QDIP, D* measured was 6.5×10^{10} cm·Hz$^{1/2}$ W^{-1} (at 77 K, 0.6 V, 7.5 μm, *f*/2). The dark current of the SK-QDIP was similar to that of the SML-QDIP operated at a bias of 0.4–0.6 V. The responsivity of SK-QDIP was measured to be ∼0.1 A/W and values of 2–6 stacks of SML-QDIP had responsivity values of ∼0.1 A/W, ∼0.08 A/W, ∼0.45 A/W ∼0.3 A/W, ∼0.1 A/W, respectively. It should be noted that a direct comparison of the value of D* cannot be made between the SK-QDIP and SML-QDIPs because the number of periods of active region is not identical in the two cases. Number of periods in the active region was 7 in the case of the SK-QDIP and 10 for the SML-QDIP. The SML-QD device was operated at a lower bias compared to the SK-QD device. The absorption QE, plotted in Fig. 3(b), was calculated from the measured responsivity, and the theoretically calculated values of photoconductive gain using the following equation: $\eta = hcR_{peak}/gq\lambda_{peak}$; where R_{peak} is the responsivity and λ_{peak} is the wavelength corresponding to the peak spectral response, and g is the photoconductive gain. The absorption QE of the 2–6 stacks SML-QDIP attains values of 0.3%, 1.1%, 10%, 5%, and 2.3%, respectively. The QDIP consisting of 4 SML-QD stacks has the highest absorption QE, due to the strongest overlap of wave functions between the two states. This measurement did not account for the substrate scattering, which can increase the absorption QE.

In order to demonstrate the effect of SML-QDs, SK-QDIP and QWIP were compared using the s-to-p polarized spectral response (see Fig. 4). We obtain the best device performance with the 4 stacks SML-QDIP. The devices were polished with 45° side facet geometry, mounted on the 45° facet holder, and wire-bonded on the pins of a leadless chip carrier (LCC). The LCC was loaded in a cryostat with a KBr window and cooled to 77 K using liquid nitrogen. The wedge coupling geometry is shown in the inset of Fig. 4. For the conventional QWIP, no s-polarized spectral response was observed since the QW has no in-plane confinement but the s/p polarized spectral response ratio of the GaAs/AlGaAs QWIP device was measured to be 2.8% which can be explained by the scattering caused by the edge of the device and the SI-GaAs substrate. The s/p ratio of 4 stacks SML-QDIP was measured to be 21.7%. which is significantly higher than SK-QDIP (13%), rendering the scattering effect negligible. The s- and p-polarized spectral responses are indicators of the infrared absorption and quantum confinement of the QD in the horizontal and vertical directions. The improved s/p ratio of SML-QDIP indicates that decreasing the base width of the dots and increasing the height of the dots improve the in-plane (TE) quantum confinement and infrared absorption. These results suggest that SML-QDIP have enhanced normal incidence absorption due to smaller QD size.

In conclusion, a comparative study of the performance of infrared photodetectors based on multiple stacked SML-

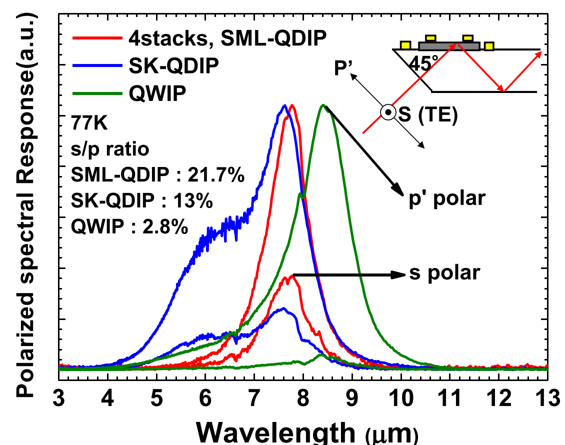

FIG. 4. Comparison of s-to-p polarized spectral response between 4 stacks SML-QDIP, SK-QDIP, and QWIP at 77 K.

Downloaded 09 Mar 2013 to 139.184.30.132. Redistribution subject to AIP license or copyright; see http://apl.aip.org/about/rights_and_permissions

QD and SK-QD is presented and also compared to results obtained with QW based detectors. The best results for detectivity and ratio of s/p polarized spectral response are obtained with the 4 stacks SML-QD device with values of 1.2×10^{11} cm·Hz$^{1/2}$ W^{-1} (at 77 K, 0.4 V, 7.5 μm, *f*/2 optics) and 21.7%, respectively. We also investigate the quantum efficiency of SML-QDIP and SK-QDIP. The multiple stacked SML-QDIPs show better performance compared to the SK QDIP with respect to the higher s/p ratio and QE due to the smaller base width of SML QD and better quantum confinement. The optical and device performance characteristics show promise in use of such devices to improve the performance of infrared focal plane arrays in the future.

This work was supported by KRISS-UNM Global Research Laboratory program (No. 2007-00011) of the National Research Foundation (NRF) of Korea and AFRL FA8718-09-C-0038. Partial funding from Department of Science and Technology, India is acknowledged. We are grateful to Jannell Vander Grift for proof-reading the manuscript.

[1]P. M. Petroff, A. Lorke, and A. Imanoglu, Phys. Today **54**(5), 46 (2001).
[2]M. Kuntz, G. Fiol, M. Laemmlin, D. Bimberg, M. G. Thompson, K. T. Tan, C. Marinelli, R. V. Penty, I. H. White, V. M. Ustinov, A. E. Zhukov, Yu. M. Shernyakov, and A. R. Kovsh, Appl. Phys. Lett. **85**, 843 (2004).
[3]I. R. Sellers, H. Y. Liu, K. M. Groom, D. T. Childs, D. Robbins, T. J. Badcock, M. Hopkinson, D. J. Mowbray, and M. S. Skolnick, Electron. Lett. **40**, 1412 (2004).
[4]J. Jiang, K. Mi, S. Tsao, W. Zhang, H. Lim, T. O'Sullivan, T. Sills, M. Razeghi, G. J. Brown, and M. Z. Tidrow, Appl. Phys. Lett. **84**, 2232 (2004).
[5]E.-T. Kim, A. Madhukar, Z. Ye, and C. Campbell, Appl. Phys. Lett. **84**, 3277 (2004).
[6]Z. Yuan, B. E. Kardynal, R. M. Stevenson, A. J. Shields, C. J. Lobo, K. Cooper, N. S. Beattie, D. A. Ritchie, and M. Pepper, Science **295**, 102 (2002).
[7]M. Jung, K. Hirakawa, Y. Kawaguchi, S. Komiyama, S. Ishida, and Y. Arakawa, Appl. Phys. Lett. **86**, 033106 (2005).
[8]P. B. Joyce and T. J. Krzyzewski, G. R. Bell, B. A. Joyce, and T. S. Jones, Phys. Rev. B **58**, R15981 (1998).
[9]Y. Koichi, Y. Kunihiko, and K. Toshiyuki, Jpn. J. Appl. Phys., Part 1 **39**, 1245 (2000).
[10]J. O. Kim, S. J. Lee, S. K. Noh, J. W. Choe, and T. W. Kang, J. Korean Phys. Soc. **53**, 2100 (2008).
[11]N. K. Cho, S. P. Ryu, J. D. Song, W. J. Choi, J. I. Lee, and Heonsu Jeon, Appl. Phys. Lett. **88**, 133104 (2006).
[12]M. Jo, T. Mano, Y. Sakuma, and K. Sakoda, Appl. Phys. Lett. **100**, 212113 (2012)
[13]F. Hopfer, A. Mutig, M. Kuntz, G. Fiol, D. Bimberg, N. N. Ledentsov, V. A. Shchukin, S. S. Mikhrin, D. L. Livshits, I. L. Krestnikov, and A. R. Kovsh, Appl. Phys. Lett. **89**, 141106 (2006).
[14]T. D. Germann, A. Strittmatter, J. Pohl, U. W. Pohl, D. Bimberg, J. Rautiainen, M. Guina, and O. G. Okhotnikov, Appl. Phys. Lett. **92**, 101123 (2008).
[15]S. Krishna, J. Phys. D: Appl. Phys. **38**(13), 2142–2150 (2005).
[16]L. Höglund, C. Asplund, Q. Wang, S. Almqvist, H. Malm, E. Petrini, J. Y. Andersson, P. O. Holtz, and H. Pettersson, Appl. Phys. Lett. **88**(21), 213510 (2006).
[17]X. Han, J. Li, J. Wu, G. Cong, X. Liu, Q. Zhu, and Z. Wang, J. Appl. Phys. **98**, 053703 (2005).
[18]A. V. Barve, S. Sengupta, J. O. Kim, Y. D. Sharma, S. Adhikary, T. J. Rotter, S. J. Lee, Y. H. Kim, and S. Krishna, Appl. Phys. Lett. **99**, 191110 (2011).
[19]X. H. Su, J. Yang, P. Bhattacharya, G. Ariyawansa, and A. G. U. Perera, Appl. Phys. Lett. **89**, 031117 (2006).
[20]D. Z.-Y. Ting, S. V. Bandara, S. D. Gunapala, J. M. Mumolo, S. A. Keo, C. J. Hill, J. K. Liu, E. R. Blazejewski, B. Rafol, and Y.-C. Chang, Appl. Phys. Lett. **94**, 111107 (2009).
[21]Z. C. Xu, D. Birkedal, J. M. Hvam, Z. Y. Zhao, Y. M. Liu, K. T. Yang, A. Kanjilal, and J. Sadowski, Appl. Phys. Lett. **82**, 3859 (2003).
[22]Z. Xu, K. Leosson, D. Birkedal, V. Lyssenko, J. M. Hvam, and J. Sadowski, Nanotechnology **14**, 1259 (2003).

Downloaded 09 Mar 2013 to 139.184.30.132. Redistribution subject to AIP license or copyright; see http://apl.aip.org/about/rights_and_permissions